Search for neutralinos scalar leptons and scalar quarks in e^+e^- interactions at $\sqrt{s} = 130$ GeV and 136 GeV

P. Abreu, W. Adam, T. Adye, E. Agasi, I. Ajinenko, G D. Alekseev, R. Alemany, P P. Allport, S. Almehed, U. Amaldi, et al.

EUROPEAN ORGANIZATION FOR NUCLEAR RESEARCH

CERN–PPE/96-110

31 July 1996

Search for neutralinos, scalar leptons and scalar quarks in e^+e^- interactions at $\sqrt{s}$=130 GeV and 136 GeV

DELPHI Collaboration

Abstract

Using data accumulated by DELPHI during the November 1995 LEP run at 130 GeV – 136 GeV, searches have been made for events with jets or leptons in conjunction with missing momentum. The results are interpreted in terms of limits on the production of neutralinos, scalar leptons, and scalar quarks.

(To be submitted to Physics Letters B)

P.Abreu[21], W.Adam[50], T.Adye[37], E.Agasi[31], I.Ajinenko[42], G.D.Alekseev[16], R.Alemany[49], P.P.Allport[22], S.Almehed[24], U.Amaldi[9], S.Amato[47], P.Andersson[44], A.Andreazza[28], M.L.Andrieux[14], P.Antilogus[9], W-D.Apel[17], B.Åsman[44], J-E.Augustin[25], A.Augustinus[9], P.Baillon[9], P.Bambade[19], F.Barao[21], R.Barate[14], M.Barbi[47], D.Y.Bardin[16], A.Baroncelli[40], O.Barring[24], J.A.Barrio[26], W.Bartl[50], M.J.Bates[37], M.Battaglia[15], M.Baubillier[23], J.Baudot[39], K-H.Becks[52], M.Begalli[6], P.Beilliere[8], Yu.Belokopytov[9,53], A.C.Benvenuti[5], M.Berggren[47], D.Bertini[25], D.Bertrand[2], M.Besancon[39], F.Bianchi[45], M.Bigi[45], M.S.Bilenky[16], P.Billoir[23], D.Bloch[10], M.Blume[52], T.Bolognese[39], M.Bonesini[28], W.Bonivento[28], P.S.L.Booth[22], C.Bosio[40], O.Botner[48], E.Boudinov[31], B.Bouquet[19], C.Bourdarios[9], T.J.V.Bowcock[22], M.Bozzo[13], P.Branchini[40], K.D.Brand[36], T.Brenke[52], R.A.Brenner[15], C.Bricman[2], R.C.A.Brown[9], P.Bruckman[18], J-M.Brunet[8], L.Bugge[33], T.Buran[33], T.Burgsmueller[52], P.Buschmann[52], A.Buys[9], S.Cabrera[49], M.Caccia[28], M.Calvi[28], A.J.Camacho Rozas[41], T.Camporesi[9], V.Canale[38], M.Canepa[13], K.Cankocak[44], F.Cao[2], F.Carena[9], L.Carroll[22], C.Caso[13], M.V.Castillo Gimenez[49], A.Cattai[9], F.R.Cavallo[5], V.Chabaud[9], Ph.Charpentier[9], L.Chaussard[25], P.Checchia[36], G.A.Chelkov[16], M.Chen[2], R.Chierici[45], P.Chliapnikov[42], P.Chochula[7], V.Chorowicz[9], J.Chudoba[30], V.Cindro[43], P.Collins[9], J.L.Contreras[19], R.Contri[13], E.Cortina[49], G.Cosme[19], F.Cossutti[46], J-H.Cowell[22], H.B.Crawley[1], D.Crennell[37], G.Crosetti[13], J.Cuevas Maestro[34], S.Czellar[15], E.Dahl-Jensen[29], J.Dahm[52], B.Dalmagne[19], M.Dam[29], G.Damgaard[29], P.D.Dauncey[37], M.Davenport[9], W.Da Silva[23], C.Defoix[8], A.Deghorain[2], G.Della Ricca[46], P.Delpierre[27], N.Demaria[35], A.De Angelis[9], W.De Boer[17], S.De Brabandere[2], C.De Clercq[2], C.De La Vaissiere[23], B.De Lotto[46], A.De Min[36], L.De Paula[47], C.De Saint-Jean[39], H.Dijkstra[9], L.Di Ciaccio[38], A.Di Diodato[38], F.Djama[10], J.Dolbeau[8], M.Donszelmann[9], K.Doroba[51], M.Dracos[10], J.Drees[52], K.-A.Drees[52], M.Dris[32], J-D.Durand[25], D.Edsall[1], R.Ehret[17], T.Ekelof[48], G.Ekspong[44], M.Elsing[52], J-P.Engel[10], B.Erzen[43], M.Espirito Santo[21], E.Falk[24], D.Fassouliotis[32], M.Feindt[9], A.Ferrer[49], S.Fichet[23], T.A.Filippas[32], A.Firestone[1], P.-A.Fischer[10], H.Foeth[9], E.Fokitis[32], F.Fontanelli[13], F.Formenti[9], B.Franek[37], P.Frenkiel[8], D.C.Fries[17], A.G.Frodesen[4], R.Fruhwirth[50], F.Fulda-Quenzer[19], J.Fuster[49], A.Galloni[22], D.Gamba[45], M.Gandelman[6], C.Garcia[49], J.Garcia[41], C.Gaspar[9], U.Gasparini[36], Ph.Gavillet[9], E.N.Gazis[32], D.Gele[10], J-P.Gerber[10], R.Gokieli[51], B.Golob[43], G.Gopal[37], L.Gorn[1], M.Gorski[51], Yu.Gouz[45,53], V.Gracco[13], E.Graziani[40], C.Green[22], A.Grefrath[52], P.Gris[39], G.Grosdidier[19], K.Grzelak[51], S.Gumenyuk[28,53], P.Gunnarsson[44], M.Gunther[48], J.Guy[37], F.Hahn[9], S.Hahn[52], Z.Hajduk[18], A.Hallgren[48], K.Hamacher[52], W.Hao[31], F.J.Harris[35], V.Hedberg[24], J.J.Hernandez[49], P.Herquet[2], H.Herr[9], T.L.Hessing[35], E.Higon[49], H.J.Hilke[9], T.S.Hill[1], S-O.Holmgren[44], P.J.Holt[35], D.Holthuizen[31], S.Hoorelbeke[2], M.Houlden[22], J.Hrubec[50], K.Huet[2], K.Hultqvist[44], J.N.Jackson[22], R.Jacobsson[44], P.Jalocha[18], R.Janik[7], Ch.Jarlskog[24], G.Jarlskog[24], P.Jarry[39], B.Jean-Marie[19], E.K.Johansson[44], L.Jonsson[24], P.Jonsson[24], C.Joram[9], P.Juillot[10], M.Kaiser[17], F.Kapusta[23], K.Karafasoulis[11], M.Karlsson[44], E.Karvelas[11], S.Katsanevas[3], E.C.Katsoufis[32], R.Keranen[4], Yu.Khokhlov[42], B.A.Khomenko[16], N.N.Khovanski[16], B.King[22], N.J.Kjaer[29], O.Klapp[52], H.Klein[9], A.Klovning[4], P.Kluit[31], B.Koene[31], P.Kokkinias[11], M.Koratzinos[9], K.Korcyl[18], V.Kostioukhine[42], C.Kourkoumelis[3], O.Kouznetsov[13,16], M.Krammer[50], C.Kreuter[17], I.Kronkvist[24], Z.Krumstein[16], W.Krupinski[18], P.Kubinec[7], W.Kucewicz[18], K.Kurvinen[15], C.Lacasta[49], I.Laktineh[25], J.W.Lamsa[1], L.Lanceri[46], D.W.Lane[1], P.Langefeld[52], V.Lapin[42], J-P.Laugier[39], R.Lauhakangas[15], G.Leder[50], F.Ledroit[14], V.Lefebure[2], C.K.Legan[1], R.Leitner[30], J.Lemonne[2], G.Lenzen[52], V.Lepeltier[19], T.Lesiak[18], J.Libby[35], D.Liko[50], R.Lindner[52], A.Lipniacka[44], I.Lippi[36], B.Loerstad[24], J.G.Loken[35], J.M.Lopez[41], D.Loukas[11], P.Lutz[39], L.Lyons[35], J.MacNaughton[50], G.Maehlum[17], J.R.Mahon[6], A.Maio[21], T.G.M.Malmgren[44], V.Malychev[16], F.Mandl[50], J.Marco[41], R.Marco[41], B.Marechal[47], M.Margoni[36], J-C.Marin[9], C.Mariotti[40], A.Markou[11], C.Martinez-Rivero[41], F.Martinez-Vidal[49], S.Marti i Garcia[22], J.Masik[30], F.Matorras[41], C.Matteuzzi[28], G.Matthiae[38], M.Mazzucato[36], M.Mc Cubbin[9], R.Mc Kay[1], R.Mc Nulty[22], J.Medbo[48], M.Merk[31], C.Meroni[28], S.Meyer[17], W.T.Meyer[1], A.Miagkov[42], M.Michelotto[36], E.Migliore[45], L.Mirabito[25], U.Mjoernmark[24], T.Moa[44], R.Moeller[29], K.Moenig[52], M.R.Monge[13], P.Morettini[13], H.Mueller[17], L.M.Mundim[6], W.J.Murray[37], B.Muryn[18], G.Myatt[35], F.Naraghi[14], F.L.Navarria[5], S.Navas[49], K.Nawrocki[51], P.Negri[28], S.Nemecek[12], W.Neumann[52], N.Neumeister[50], R.Nicolaidou[3], B.S.Nielsen[29], M.Nieuwenhuizen[31], V.Nikolaenko[10], P.Niss[44], A.Nomerotski[36], A.Normand[35], W.Oberschulte-Beckmann[17], V.Obraztsov[42], A.G.Olshevski[16], A.Onofre[21], R.Orava[15], K.Osterberg[15], A.Ouraou[39], P.Paganini[19], M.Paganoni[9,28], P.Pages[10], R.Pain[23], H.Palka[18], Th.D.Papadopoulou[32], K.Papageorgiou[11], L.Pape[9], C.Parkes[35], F.Parodi[13], A.Passeri[40], M.Pegoraro[36], L.Peralta[21], H.Pernegger[50], M.Pernicka[50], A.Perrotta[5], C.Petridou[46], A.Petrolini[13], M.Petrovyck[42], H.T.Phillips[37], G.Piana[13], F.Pierre[39], M.Pimenta[21], S.Plaszczynski[19], O.Podobrin[17], M.E.Pol[6], G.Polok[18], P.Poropat[46], V.Pozdniakov[16], P.Privitera[38], N.Pukhaeva[16], A.Pullia[28], D.Radojicic[35], S.Ragazzi[28], H.Rahmani[32], P.N.Ratoff[20], A.L.Read[33], M.Reale[52], P.Rebecchi[19], N.G.Redaelli[28], M.Regler[50], D.Reid[9], P.B.Renton[35], L.K.Resvanis[3], F.Richard[19], J.Richardson[22], J.Ridky[12], G.Rinaudo[45], I.Ripp[39], A.Romero[45], I.Roncagliolo[13], P.Ronchese[36], L.Roos[14], E.I.Rosenberg[1], E.Rosso[9], P.Roudeau[19], T.Rovelli[5], W.Ruckstuhl[31], V.Ruhlmann-Kleider[39], A.Ruiz[41], K.Rybicki[18], H.Saarikko[15], Y.Sacquin[39], A.Sadovsky[16], O.Sahr[14], G.Sajot[14], J.Salt[49], J.Sanchez[26], M.Sannino[13], M.Schimmelpfennig[17], H.Schneider[17], U.Schwickerath[17], M.A.E.Schyns[52], G.Sciolla[45], F.Scuri[46], P.Seager[20], Y.Sedykh[16], A.M.Segar[35], A.Seitz[17], R.Sekulin[37], L.Serbelloni[38], R.C.Shellard[6], I.Siccama[31], P.Siegrist[39], R.Silvestre[39], S.Simonetti[39], F.Simonetto[36], A.N.Sisakian[16], B.Sitar[7], T.B.Skaali[33], G.Smadja[25], N.Smirnov[42], O.Smirnova[24], G.R.Smith[37], A.Sokolov[42], R.Sosnowski[51], D.Souza-Santos[6], T.Spassov[21], E.Spiriti[40], P.Sponholz[52], S.Squarcia[13], C.Stanescu[40], S.Stapnes[33], I.Stavitski[36], K.Stevenson[35], F.Stichelbaut[9], A.Stocchi[19], J.Strauss[50], R.Strub[10], B.Stugu[4], M.Szczekowski[51], M.Szeptycka[51], T.Tabarelli[28], J.P.Tavernet[23],

E.Tcherniaev[42], O.Tchikilev[42], J.Thomas[35], A.Tilquin[27], J.Timmermans[31], L.G.Tkatchev[16], T.Todorov[10], S.Todorova[10], D.Z.Toet[31], A.Tomaradze[2], B.Tome[21], A.Tonazzo[28], L.Tortora[40], G.Transtromer[24], D.Treille[9], W.Trischuk[9], G.Tristram[8], A.Trombini[19], C.Troncon[28], A.Tsirou[9], M-L.Turluer[39], I.A.Tyapkin[16], M.Tyndel[37], S.Tzamarias[22], B.Ueberschaer[52], O.Ullaland[9], V.Uvarov[42], G.Valenti[5], E.Vallazza[9], C.Vander Velde[2], G.W.Van Apeldoorn[31], P.Van Dam[31], J.Van Eldik[31], N.Vassilopoulos[35], G.Vegni[28], L.Ventura[36], W.Venus[37], F.Verbeure[2], M.Verlato[36], L.S.Vertogradov[16], D.Vilanova[39], P.Vincent[25], L.Vitale[46], E.Vlasov[42], A.S.Vodopyanov[16], V.Vrba[12], H.Wahlen[52], C.Walck[44], F.Waldner[46], M.Weierstall[52], P.Weilhammer[9], C.Weiser[17], A.M.Wetherell[9], D.Wicke[52], J.H.Wickens[2], M.Wielers[17], G.R.Wilkinson[35], W.S.C.Williams[35], M.Winter[10], M.Witek[18], K.Woschnagg[48], K.Yip[35], O.Yushchenko[42], F.Zach[25], A.Zaitsev[42], A.Zalewska[9], P.Zalewski[51], D.Zavrtanik[43], E.Zevgolatakos[11], N.I.Zimin[16], M.Zito[39], D.Zontar[43], G.C.Zucchelli[44], G.Zumerle[36]

[1] Department of Physics and Astronomy, Iowa State University, Ames IA 50011-3160, USA
[2] Physics Department, Univ. Instelling Antwerpen, Universiteitsplein 1, B-2610 Wilrijk, Belgium
and IIHE, ULB-VUB, Pleinlaan 2, B-1050 Brussels, Belgium
and Faculté des Sciences, Univ. de l'Etat Mons, Av. Maistriau 19, B-7000 Mons, Belgium
[3] Physics Laboratory, University of Athens, Solonos Str. 104, GR-10680 Athens, Greece
[4] Department of Physics, University of Bergen, Allégaten 55, N-5007 Bergen, Norway
[5] Dipartimento di Fisica, Università di Bologna and INFN, Via Irnerio 46, I-40126 Bologna, Italy
[6] Centro Brasileiro de Pesquisas Físicas, rua Xavier Sigaud 150, RJ-22290 Rio de Janeiro, Brazil
and Depto. de Física, Pont. Univ. Católica, C.P. 38071 RJ-22453 Rio de Janeiro, Brazil
and Inst. de Física, Univ. Estadual do Rio de Janeiro, rua São Francisco Xavier 524, Rio de Janeiro, Brazil
[7] Comenius University, Faculty of Mathematics and Physics, Mlynska Dolina, SK-84215 Bratislava, Slovakia
[8] Collège de France, Lab. de Physique Corpusculaire, IN2P3-CNRS, F-75231 Paris Cedex 05, France
[9] CERN, CH-1211 Geneva 23, Switzerland
[10] Centre de Recherche Nucléaire, IN2P3 - CNRS/ULP - BP20, F-67037 Strasbourg Cedex, France
[11] Institute of Nuclear Physics, N.C.S.R. Demokritos, P.O. Box 60228, GR-15310 Athens, Greece
[12] FZU, Inst. of Physics of the C.A.S. High Energy Physics Division, Na Slovance 2, 180 40, Praha 8, Czech Republic
[13] Dipartimento di Fisica, Università di Genova and INFN, Via Dodecaneso 33, I-16146 Genova, Italy
[14] Institut des Sciences Nucléaires, IN2P3-CNRS, Université de Grenoble 1, F-38026 Grenoble Cedex, France
[15] Research Institute for High Energy Physics, SEFT, P.O. Box 9, FIN-00014 Helsinki, Finland
[16] Joint Institute for Nuclear Research, Dubna, Head Post Office, P.O. Box 79, 101 000 Moscow, Russian Federation
[17] Institut für Experimentelle Kernphysik, Universität Karlsruhe, Postfach 6980, D-76128 Karlsruhe, Germany
[18] Institute of Nuclear Physics and University of Mining and Metalurgy, Ul. Kawiory 26a, PL-30055 Krakow, Poland
[19] Université de Paris-Sud, Lab. de l'Accélérateur Linéaire, IN2P3-CNRS, Bât. 200, F-91405 Orsay Cedex, France
[20] School of Physics and Chemistry, University of Lancaster, Lancaster LA1 4YB, UK
[21] LIP, IST, FCUL - Av. Elias Garcia, 14-1^{o}, P-1000 Lisboa Codex, Portugal
[22] Department of Physics, University of Liverpool, P.O. Box 147, Liverpool L69 3BX, UK
[23] LPNHE, IN2P3-CNRS, Universités Paris VI et VII, Tour 33 (RdC), 4 place Jussieu, F-75252 Paris Cedex 05, France
[24] Department of Physics, University of Lund, Sölvegatan 14, S-22363 Lund, Sweden
[25] Université Claude Bernard de Lyon, IPNL, IN2P3-CNRS, F-69622 Villeurbanne Cedex, France
[26] Universidad Complutense, Avda. Complutense s/n, E-28040 Madrid, Spain
[27] Univ. d'Aix - Marseille II - CPP, IN2P3-CNRS, F-13288 Marseille Cedex 09, France
[28] Dipartimento di Fisica, Università di Milano and INFN, Via Celoria 16, I-20133 Milan, Italy
[29] Niels Bohr Institute, Blegdamsvej 17, DK-2100 Copenhagen 0, Denmark
[30] NC, Nuclear Centre of MFF, Charles University, Areal MFF, V Holesovickach 2, 180 00, Praha 8, Czech Republic
[31] NIKHEF-H, Postbus 41882, NL-1009 DB Amsterdam, The Netherlands
[32] National Technical University, Physics Department, Zografou Campus, GR-15773 Athens, Greece
[33] Physics Department, University of Oslo, Blindern, N-1000 Oslo 3, Norway
[34] Dpto. Fisica, Univ. Oviedo, C/P. Pérez Casas, S/N-33006 Oviedo, Spain
[35] Department of Physics, University of Oxford, Keble Road, Oxford OX1 3RH, UK
[36] Dipartimento di Fisica, Università di Padova and INFN, Via Marzolo 8, I-35131 Padua, Italy
[37] Rutherford Appleton Laboratory, Chilton, Didcot OX11 OQX, UK
[38] Dipartimento di Fisica, Università di Roma II and INFN, Tor Vergata, I-00173 Rome, Italy
[39] CEA, DAPNIA/Service de Physique des Particules, CE-Saclay, F-91191 Gif-sur-Yvette Cedex, France
[40] Istituto Superiore di Sanità, Ist. Naz. di Fisica Nucl. (INFN), Viale Regina Elena 299, I-00161 Rome, Italy
[41] Instituto de Fisica de Cantabria (CSIC-UC), Avda. los Castros, S/N-39006 Santander, Spain, (CICYT-AEN93-0832)
[42] Inst. for High Energy Physics, Serpukov P.O. Box 35, Protvino, (Moscow Region), Russian Federation
[43] J. Stefan Institute and Department of Physics, University of Ljubljana, Jamova 39, SI-61000 Ljubljana, Slovenia
[44] Fysikum, Stockholm University, Box 6730, S-113 85 Stockholm, Sweden
[45] Dipartimento di Fisica Sperimentale, Università di Torino and INFN, Via P. Giuria 1, I-10125 Turin, Italy
[46] Dipartimento di Fisica, Università di Trieste and INFN, Via A. Valerio 2, I-34127 Trieste, Italy
and Istituto di Fisica, Università di Udine, I-33100 Udine, Italy
[47] Univ. Federal do Rio de Janeiro, C.P. 68528 Cidade Univ., Ilha do Fundão BR-21945-970 Rio de Janeiro, Brazil
[48] Department of Radiation Sciences, University of Uppsala, P.O. Box 535, S-751 21 Uppsala, Sweden
[49] IFIC, Valencia-CSIC, and D.F.A.M.N., U. de Valencia, Avda. Dr. Moliner 50, E-46100 Burjassot (Valencia), Spain
[50] Institut für Hochenergiephysik, Österr. Akad. d. Wissensch., Nikolsdorfergasse 18, A-1050 Vienna, Austria
[51] Inst. Nuclear Studies and University of Warsaw, Ul. Hoza 69, PL-00681 Warsaw, Poland
[52] Fachbereich Physik, University of Wuppertal, Postfach 100 127, D-42097 Wuppertal, Germany
[53] On leave of absence from IHEP Serpukhov

1 Introduction

Supersymmetric partners of neutral gauge bosons (gauginos) and neutral Higgs states (Higgsinos) are postulated in supersymmetric extensions of the Standard Model [1]. In the Minimal Supersymmetric extension (the MSSM) these are realized in four neutralino mass states, $\tilde{\chi}_i^0$, $i = 1, 4$, which are linear superpositions of gaugino and Higgsino eigenstates and are expected to be produced at LEP in $\tilde{\chi}_i^0\tilde{\chi}_j^0$ pairs. The lightest neutralino, $\tilde{\chi}_1^0$, is usually assumed to be the lightest supersymmetric particle. This assumption, along with that of conserved R-parity, was made for the analysis presented in this paper. An implication of this is that $\tilde{\chi}_1^0$ is stable and undetectable because it interacts only weakly.

Channels such as $e^+e^- \rightarrow \tilde{\chi}_1^0\tilde{\chi}_2^0$ or $\tilde{\chi}_2^0\tilde{\chi}_2^0$ are visible, however, with the second lightest neutralino, $\tilde{\chi}_2^0$, decaying into $\tilde{\chi}_1^0$ and a fermion-antifermion pair or a photon, giving events characterised by missing energy and momentum. This would be most striking in the case of $\tilde{\chi}_1^0\tilde{\chi}_2^0$, which is also kinematically favoured. Limits on their production at LEP have been set previously, based on data taken at the Z^0 resonance [2].

Neutralinos are produced through s-channel Z^0 exchange and t-channel exchange of scalar electrons. The present analysis is primarily sensitive to Higgsino-dominated light neutralinos which would have large cross sections because of the large coupling between the Higgsino and the Z^0. In the MSSM, with a common gaugino mass at the GUT scale, neutralinos are Higgsino-like when the $SU(2)_L$ gaugino mass parameter, M_2, is large compared to the Higgs superfield mass parameter $|\mu|$. It is noteworthy that in this case there is little dependence on the common MSSM scalar mass term m_0, i.e. the cross section depends essentially on three parameters: M_2, μ, and the ratio of the vacuum expectation values of the two Higgs doublets, $\tan\beta$.

Scalar leptons (sleptons) are pair-produced through Z^0/γ exchange in the s-channel. In addition, t-channel neutralino exchange contributes to selectron production and it can enhance the selectron production in some regions of the MSSM parameter space. Because of the small electron and muon masses, mixing between the scalar partners of the two chirality states is expected to be negligible, and the expected final states are $\tilde{\ell}_R\bar{\tilde{\ell}}_R$ and $\tilde{\ell}_L\bar{\tilde{\ell}}_L$ ($\tilde{\ell} = \tilde{\mu}, \tilde{\mathrm{e}}$). But because of the t-channel contribution, the channel $\tilde{\mathrm{e}}_L\tilde{\mathrm{e}}_R$ may also have a significant cross section even if there is no selectron mixing. Sleptons are expected to decay according to $\tilde{\ell} \rightarrow \ell\tilde{\chi}_1^0$, giving events with two leptons acoplanar with the beam axis, missing energy, and missing momentum.

The supersymmetric partner of the top quark (the stop, $\tilde{\mathrm{t}}$) could be the lightest scalar quark. Because of the large mass of the top quark, the scalar partners of its two chirality states, $\tilde{\mathrm{t}}_R$ and $\tilde{\mathrm{t}}_L$, are expected to mix [3], and the lighter physical state could be significantly below the typical mass of scalar quarks and hence accessible at LEP. In the MSSM, a sufficiently light $\tilde{\mathrm{t}}$ could contribute, through virtual corrections, to the large measured partial width $\Gamma(\mathrm{Z}^0 \rightarrow \mathrm{b\bar{b}})$ as compared to the Standard Model prediction [4,5]. The $\tilde{\mathrm{t}}$ is expected to decay into $\mathrm{b}\tilde{\chi}_1^+$ if kinematically allowed, otherwise into $\mathrm{c}\tilde{\chi}_1^0$, in both cases with a branching ratio close to unity. The negative result of chargino searches [6,7] implies the former channel is closed at present energies. Therefore the present analysis considers only the $\mathrm{c}\tilde{\chi}_1^0$ decay. This leads to events with two jets, missing energy, and missing momentum, similar to the $\tilde{\chi}_1^0\tilde{\chi}_2^0$ final state.

The sbottom or scalar bottom quarks, $\tilde{\mathrm{b}}_R$ and $\tilde{\mathrm{b}}_L$, could also mix significantly if $\tan\beta$ is large (about 10 or greater). In this case the lighter physical $\tilde{\mathrm{b}}$ state could be the lightest scalar quark. The $\tilde{\mathrm{b}}$ is expected to decay into $\mathrm{b}\tilde{\chi}_1^0$, giving a signature similar to that for the stop.

This paper presents a search for neutralinos, scalar quarks and scalar leptons in the data accumulated by DELPHI in the first high energy run of LEP in November 1995. Similar searches have been performed by other LEP experiments [7]. The paper is organised as follows: Section 2 gives a brief description of the detector, section 3 describes the real data and the simulated signal and background samples, while section 4 describes the analyses applied for the different topologies. Section 5 gives the results of the selections and their interpretation. Section 6 contains the conclusions.

2 Detector description

The following is a summary of the properties of the DELPHI detector [8] relevant to this analysis. Charged particle tracks were reconstructed in the 1.2 T solenoidal magnetic field by a system of cylindrical tracking chambers. These were the Microvertex Detector (VD), the Inner Detector (ID), the Time Projection Chamber (TPC), and the Outer Detector (OD). In addition, two planes of drift chambers aligned perpendicular to the beam axis (Forward Chambers A and B) tracked particles in the forward and backward directions, covering polar angles $11^\circ < \theta < 33^\circ$ and $147^\circ < \theta < 169^\circ$ with respect to the beam (z) direction.

The VD consisted of three cylindrical layers of silicon detectors, at radii 6.3 cm, 9.0 cm and 11.0 cm. All three layers measured coordinates in the plane transverse to the beam. The closest (6.3 cm) and the outer (11.0 cm) layers contained double-sided detectors to measure also z coordinates. The polar angle coverage of the VD was from 25° to 155° for the closest and from 44° to 136° for the outer layer. The ID was a cylindrical drift chamber (inner radius 12 cm and outer radius 22 cm) covering polar angles between 15° and 165°. The TPC, the principal tracking device of DELPHI, was a cylinder of 30 cm inner radius, 122 cm outer radius and had a length of 2.7 m. Each end-plate was divided into 6 sectors, with 192 sense wires used for the dE/dx measurement and 16 circular pad rows used for 3 dimensional space-point reconstruction. The OD consisted of 5 layers of drift cells at radii between 192 cm and 208 cm, covering polar angles between 43° and 137°.

The average momentum resolution for the charged particles in hadronic final states was in the range $\Delta p/p^2 \simeq 0.001$ to 0.01 $(\mathrm{GeV}/c)^{-1}$, depending on which detectors were used in the track fit [8].

The electromagnetic calorimeters were the High density Projection Chamber (HPC) covering the barrel region of $40^\circ < \theta < 140^\circ$, the Forward ElectroMagnetic Calorimeter (FEMC) covering $11^\circ < \theta < 36^\circ$ and $144^\circ < \theta < 169^\circ$, and the STIC, a Scintillator TIle Calorimeter which extended coverage down to 1.66° from the beam axis in either direction. The 40° taggers were a series of single layer scintillator-lead counters used to veto electromagnetic particles that would otherwise be missed in the region between the HPC and FEMC. The efficiency to register a photon with energy above 5 GeV measured with the LEP1 data was above 99%. The hadron calorimeter (HCAL) covered 98% of the solid angle. Muons with momenta above 2 GeV penetrated the HCAL and were recorded in a set of Muon Drift Chambers.

3 Data samples and event generators

The integrated luminosities accumulated were 2.92 pb^{-1} and 3.01 pb^{-1} at centre-of-mass energies of 130.4 GeV and 136.3 GeV respectively, and 0.04 pb^{-1} at 140 GeV.

To evaluate the signal efficiency and background contamination, events were generated using several different programs, all relying on JETSET 7.4 [9] for quark fragmentation.

The program SUSYGEN [10] was used to generate neutralino events and to calculate cross sections and branching ratios. It was verified that the result obtained agreed with the calculations of ref [11]. SUSYGEN was also used to generate the $\tilde{\ell}^+\tilde{\ell}^-$ signals. The $\tilde{\mathrm{t}}\bar{\tilde{\mathrm{t}}}$ signal was generated with a program based on the BASES/SPRING package [12], with gluon radiation treated according to [13], and intermediate $\tilde{\mathrm{t}}$-hadron fragmentation [14] [†] In this channel SUSYGEN was used as a cross check. A modified version of the BASES/SPRING generator was used for the $\tilde{\mathrm{b}}\bar{\tilde{\mathrm{b}}}$ channel.

The background processes $\mathrm{e^+e^-} \to \mathrm{f\bar{f}}(n\gamma)$ and processes leading to four-fermion final states $(\mathrm{Z^0}/\gamma)^*(\mathrm{Z^0}/\gamma)^*$, $\mathrm{W^{+*}W^{-*}}$, $\mathrm{We}\nu_\mathrm{e}$, and $\mathrm{Z^0e^+e^-}$ were generated using PYTHIA [9]. The cut on the invariant mass of the virtual $(\mathrm{Z^0}/\gamma)^*$ in the $(\mathrm{Z^0}/\gamma)^*(\mathrm{Z^0}/\gamma)^*$ process was set at 3 GeV/c^2, in order to determine the background from low mass $\mathrm{f\bar{f}}$ pairs. The calculation of the four-fermion background was verified using the program EXCALIBUR [15], which consistently takes into account all amplitudes leading to a given four-fermion final state. EXCALIBUR does not, however, include the transverse momentum of initial state radiation. Two-photon interactions leading to hadronic and leptonic final states were generated using TWOGAM [16].

Generated signal and background events were passed through detailed detector response simulation [8] and processed with the same reconstruction and analysis program as the real data. The number of background events simulated was similar to, or in most cases several times larger than, the number expected in the real data.

4 Event selections

Criteria to select events were defined on the basis of simulated signal and background events. The goal was to optimize the efficiency for wide ranges of the masses of the supersymmetric particles (see Tables 2, 3, and 4) while reducing the background expected in each search channel to the order of one event or less (see Table 1).

4.1 Two jets and missing momentum

Events with two jets and missing momentum would result from production of $\tilde{\chi}^0_1\tilde{\chi}^0_2$ with hadronic decays of $\tilde{\chi}^0_2$ or from $\tilde{\mathrm{t}}\bar{\tilde{\mathrm{t}}}$ or $\tilde{\mathrm{b}}\bar{\tilde{\mathrm{b}}}$ production.

Charged particles were selected as reconstructed tracks having momentum above 100 MeV/c, impact parameters below 5 cm in the transverse plane and 8 cm in the beam direction, and measured length greater than 30 cm or at least one associated VD point. In the forward region, a track element from the ID, the VD, or the TPC was also required. Neutral particles were selected as clusters of energy in the calorimeters, unassociated with charged particles, and with an energy above 100 MeV.

The following selection was applied to the data in order to extract a possible signal:

1. The number of charged particles was required to be at least five, with at least one particle originating within 200 μm from the interaction point in the $R\phi$ plane. These criteria selected $\mathrm{e^+e^-}$ interactions giving multihadronic final states.
2. The total energy of particles with polar angle below 30° was required to be smaller than 20% of the total visible energy, the polar angle of the missing momentum

[†] The DELPHI generator described in [14] was modified to use the intermediate $\tilde{\mathrm{t}}$-hadron fragmentation of the OPAL generator [14].

to satisfy $10^\circ < \theta_{p_{\rm miss}} < 170^\circ$, and the transverse missing momentum to exceed 5 GeV/c. These criteria served to remove two-photon interactions and $Z^0\gamma$ events.

3. The invariant mass of visible particles was required to be less than $0.55\times E_{\rm cms}$, and the missing mass had to exceed $0.35\times E_{\rm cms}$. This suppressed mainly $e^+e^- \rightarrow q\bar{q}(\gamma)$ events.
4. The number of jets reconstructed using the JADE algorithm [17], modified to use a cut on the minimal invariant mass of two jets, $y_{\rm min} = 10$ GeV/c^2, was required to be two or less, and at least one charged particle was required in each jet. The parameter choice in the jet definition allowed for the gluon emission characteristic of scalar particles [18], thus giving a high efficiency for scalar quarks.
5. Events with isolated particles, including τ leptons and photons which were often reconstructed as several close tracks, were rejected by requiring that any neutral particle with energy greater than 5 GeV should be accompanied by at least 2.5 GeV from other particles within a double cone from 5° to 25° around its momentum direction. Similarly, it was required that there be no isolated charged particle with energy greater than 10 GeV and energy in the double cone below 5 GeV. Events with an isolated signal recorded in the 40° taggers (see section 2) and with the missing momentum pointing to it were also rejected. These criteria rejected events with isolated particles and with radiated photons recorded in the detector.
6. In order to eliminate the residual background from two-photon events and Z^0 events, the events were forced to two jets using the algorithm mentioned above, and the 'scaled acoplanarity' was defined as the complement of the angle between the two jets in the transverse plane multiplied by the minimum $\sin\theta_{\rm jet}$. The scaled acoplanarity was required to be larger than 10° . The factor $\sin\theta_{\rm jet}$ accounted for the worse definition of the acoplanarity in events with jets at low polar angles.

No event satisfied these criteria. The number of background events expected from Standard Model processes is 1.0 ± 0.2 (see Table 1). The upper plot in Fig. 1 shows the acoplanarity distribution prior to the final requirement of a minimum acoplanarity for data events and simulated background events. Expected distributions for $\tilde{\chi}^0_1\tilde{\chi}^0_2$ and $\tilde{t}_L\bar{\tilde{t}}_L$ events are also shown, with the latter signal normalised to the predicted cross section.

4.2 Two jets and missing momentum using discriminant methods

An alternative procedure was applied to search specifically for $\tilde{b}\bar{\tilde{b}}$ production.

Events were selected if they had more than three charged particles, more than 5 GeV/c of missing transverse momentum, visible mass below 70 GeV/c^2, and visible energy below 100 GeV. The polar angle of the missing momentum was required to be between 20° and 160° and the total visible energy in this angular region had to exceed 15 GeV. The JADE algorithm [17] was used to cluster particles into exactly two jets, which were then required to be more than 20° away from the beam axis.

A linear discriminant analysis [19] was then used in order to optimize signal efficiencies with respect to the background. Based on the simulated data, this determined the linear combination of the variables best discriminating the $\tilde{b}$ signal sample from the Standard Model background sample. About 19000 fully simulated $\tilde{b}$ events covering different $M_{\tilde{b}}M_{\tilde{\chi}^0_1}$ configurations were used to find the best linear combination of six variables (energy and momentum of the most energetic jet, missing transverse momentum, total

multiplicity, mass of the second most energetic jet, and the second Fox-Wolfram moment [20]). This was then used for the final selection.

This procedure selected one event, consisting of two jets with energies of 13.2 GeV and 9.8 GeV, respectively, and missing transverse momentum of 6.2 GeV/c. No secondary vertices, expected from b quark decays following sbottom production, were found in this event. The number of background events expected is 2.4 ± 0.5 (see Table 1). In the analysis described in the previous section, the event was rejected by the minimum acoplanarity requirement (requirement 6 of section 4.1).

4.3 Multijets, or jets and a pair of isolated leptons, with missing energy

Events with four fermions, at least two of which are quarks, together with missing energy, could signal pair production of the second lightest neutralino according to $e^+e^- \to \tilde{\chi}^0_2\tilde{\chi}^0_2$ with one $\tilde{\chi}^0_2$ decaying into $\tilde{\chi}^0_1 q\bar{q}$ and the other into either $\tilde{\chi}^0_1 q\bar{q}$ or $\tilde{\chi}^0_1 \ell^+\ell^-$.

The charged and neutral particles were selected as in section 4.1, and the same event variables and jet definitions were used. The signal consists of multijet events ($q\bar{q}q'\bar{q}'$) or hadronic events with isolated lepton tracks ($q\bar{q}\ell^+\ell^-$), in association with missing energy and missing momentum from the escaping neutralinos. Such events were selected as follows:

1. The number of charged particles was required to be at least five, the multiplicity including neutrals had to be seven or larger, and there had to be at least one track originating within 200 μm of the interaction point. These criteria selected multihadronic e^+e^- interactions.
2. The total energy of particles within 30° of the beam axis was required to be less than 20% of the total visible energy. The missing momentum was required to be outside this polar angle range. Events with an isolated signal registered in the 40° taggers (see section 2) and with the missing momentum pointing to it were rejected. These criteria removed two-photon events and radiative Z^0 events.
3. If the event contained no isolated particle (charged or neutral) above 5 GeV and with the energy inside the double cone of section 4.1 below 3 GeV, the following selection was applied ($q\bar{q}q'\bar{q}'$ case) :
   - the transverse missing momentum was required to exceed 5 GeV/c,
   - the invariant mass of visible particles was required to be less than $0.65 \times E_{\rm cms}/c^2$,
   - the missing mass had to be greater than $0.55 \times E_{\rm cms}/c^2$,
   - the scaled acoplanarity angle between the two highest energy jets (see subsection 4.1) was required to be greater than 16°.

   If there was such a particle the following selection was used instead ($q\bar{q}\ell^+\ell^-$ case):
   - it was required that there be be at least one isolated charged particle in the polar angle interval $|\cos(\theta)| < 0.8$ reconstructed in the TPC and with more than 10% of the total visible energy, and that the energy inside the double cone for this track be below 1 GeV,
   - the transverse missing momentum was required to exceed 2.5 GeV/c,
   - the invariant mass of visible particles had to be less than $0.65 \times E_{\rm cms}/c^2$ for an event to be accepted (to reject τ background this value was reduced to $0.35 \times E_{\rm cms}/c^2$ for events with five charged particles),
   - the scaled acoplanarity angle of the two highest energy jets (see subsection 4.1) was required to be greater than 10°.

No events satisfied these criteria. The number expected from background is 0.5 ± 0.1 (see Table 1).

4.4 Two leptons and missing momentum

The topology of two leptons and missing momentum could arise from $\tilde{\chi}^0_1\tilde{\chi}^0_2$ production with $\tilde{\chi}^0_2 \to \tilde{\chi}^0_1\ell^+\ell^-$ or from $\tilde{\ell}^+\tilde{\ell}^-$ production with subsequent decay : $\tilde{\ell}^\pm \to \ell^\pm\tilde{\chi}^0_1$.

Events were selected by requiring exactly two charged particles with momenta above 1 GeV/c, polar angles in the range $20^\circ < \theta < 160^\circ$, and satisfying the following criteria.

- Both tracks had to have at least 4 TPC pad signals used in the reconstruction. The relative momentum errors ($\delta p/p$) had to be below 0.5, and the reconstructed impact parameters of the tracks in the two planes perpendicular to and containing the beam had to be below 5 cm. One or more of the tracks had to be at least loosely identified as an electron or a muon according to [8].
- No more than 2 GeV of energy in charged particles should be reconstructed within 10° of any of the two selected tracks.

For events where two such tracks were found, the following selections were applied.

- The missing energy of the event should exceed 55 GeV.
- The total multiplicity of the event had to be less than eight. The transverse momentum of the pair of particles had to exceed 6 GeV/c if the missing energy of the event was below 100 GeV, otherwise 4 GeV/c. These two different requirements were optimised for low and high $M_{\tilde{\chi}^0_1}$, respectively. In addition, the missing transverse momentum of the event had to exceed 4 GeV/c, and the energy carried by neutral particles had to be below 12 GeV. These requirements rejected background from $e^+e^- \to q\bar{q}(\gamma)$ events and two-photon interactions.
- The acollinearity and acoplanarity between the two selected particles had to exceed 8° and 12° respectively, and the invariant mass of the pair had to be below 70 GeV/c^2. These requirements rejected $e^+e^- \to e^+e^-$ events.

One event passed the selection described above. The final state consists of an e^+e^- pair with an invariant mass of 4.6 GeV/c^2 and a scalar sum of momenta of 19 GeV/c. The large acoplanarity (170°) and the large missing p_T (15 GeV/c) are not consistent with the expectation for the two-photon or radiative Bhabha backgrounds. However, the event is consistent with the background of 0.6 ± 0.3 events expected from the four-fermion process $e^+e^- \to \ell^+\ell^-\nu\bar{\nu}$ (see Table 1).

Figure 1 (lower part) shows the acoplanarity distribution for the data and the simulated background after two different selections. The first selection includes events with two good isolated tracks, low multiplicity and missing transverse momentum above 4 GeV/c. The second one includes those events which pass the selection when the final requirements on acollinearity and acoplanarity are removed. For the second selection the distribution for simulated signal events, normalised to a cross-section of 1 pb, is also shown.

4.5 Four leptons and missing energy

Events with four leptons and missing energy could be the result of $\tilde{\chi}^0_2\tilde{\chi}^0_2$ production followed by the decay $\tilde{\chi}^0_2 \to \tilde{\chi}^0_1\ell^+\ell^-$.

The selection used was similar to that of section 4.4. It was required that there be three or four isolated tracks with $20^\circ < \theta < 160^\circ$. Each had to have at least four TPC

pad signals used in the reconstruction, and at least one associated hit in the VD. The invariant masses of all two-particle combinations of these particles should be less than 90 GeV/c^2, and at least two of the particles should be identified leptons.

In addition, the missing energy of the event was required to exceed 50 GeV, the missing transverse momentum to be greater than 3 GeV/c, and the total multiplicity to be smaller than 10. The energy deposited by neutral particles was required to be smaller than 30 GeV.

No events which satisfied these requirements were found. The number expected from Standard Model processes is $0.2^{+1.1}_{-0.2}$.

5 Results

Table 1 summarises the number of accepted events in the data for the different selections. Also shown are the expected numbers of events from the different background channels.

Selection:	section 4.1	section 4.2	section 4.3	section 4.4	section 4.5
Channel:	$q\bar{q}$(A)	$q\bar{q}$(B)	$q\bar{q}\ell^+\ell^-$+$q\bar{q}q\bar{q}$	$\ell^+\ell^-$	$\ell^+\ell^-\ell^+\ell^-$
Observed events	0	1	0	1	0
Total background	1.0±0.2	2.4±0.5	0.5±0.1	$1.3^{+0.9}_{-0.4}$	$0.2^{+1.1}_{-0.2}$
$Z^0/\gamma \to ff(n\gamma)$	0.58±0.13	0	0.38±0.11	0.26±0.26	$0.0^{+0.6}_{-0.0}$
4-fermion events	0.05±0.03	0.2±0.14	0.07±0.05	0.6±0.3	$0.0^{+0.3}_{-0.0}$
$\gamma\gamma \to \tau^+\tau^-$	0.1±0.1	0	0	0.45±0.16	0.15±0.16
$\gamma\gamma \to e^+e^-, \mu^+\mu^-$	0	0	0	$0.0^{+0.8}_{-0.0}$	$0.0^{+0.8}_{-0.0}$
$\gamma\gamma \to$ *hadrons*	0.23±0.11	2.2±0.4	0.06±0.03	$0.0^{+0.4}_{-0.0}$	$0.0^{+0.4}_{-0.0}$

Table 1: The number of events observed in each search channel, together with the total number of background events expected and the numbers expected from the individual background sources. When a quoted symmetric error range would extend below zero events truncation at zero is implied.

5.1 Results on neutralino production

To determine the efficiency as a function of the neutralino masses, events were generated using `SUSYGEN` for different values of $M_{\tilde{\chi}^0_1}$ and $M_{\tilde{\chi}^0_2} - M_{\tilde{\chi}^0_1}$, and for different decay channels. A total of 54000 $\tilde{\chi}^0_1\tilde{\chi}^0_2$ events were passed through the DELPHI full detector simulation [8] and event reconstruction programs. The selections described above were then applied to these events. Table 2 shows the selection efficiencies determined by this procedure for three $\tilde{\chi}^0_2$ decay modes. There is a small difference between the efficiencies for different relative CP sign of $\tilde{\chi}^0_1$ and $\tilde{\chi}^0_2$, the lower value is quoted in the table. The systematic errors are about ±2% absolute and were subtracted from the efficiencies quoted when calculating limits.

For each combination of masses each of these efficiencies may be used, together with the observed number of events and expected background, to derive an upper limit on the corresponding product of cross section and branching ratio of a specific decay [21]. For the background, a conservative lower limit was used (0.2 events in the two lepton channel, zero in the other channels). The single candidate in the $\tilde{\chi}^0_1\tilde{\chi}^0_2$ electron channel was included in

Mass (GeV/c^2)		Efficiency (%)			Mass (GeV/c^2)		Efficiency (%)		
$M_{\tilde{\chi}^0_1}$	$M_{\tilde{\chi}^0_2}$	$\tilde{\chi}^0_1 e^+e^-$	$\tilde{\chi}^0_1 \mu^+\mu^-$	$\tilde{\chi}^0_1 q\bar{q}$	$M_{\tilde{\chi}^0_1}$	$M_{\tilde{\chi}^0_2}$	$\tilde{\chi}^0_1 e^+e^-$	$\tilde{\chi}^0_1 \mu^+\mu^-$	$\tilde{\chi}^0_1 q\bar{q}$
15	75	51	65	47	40	50	50	61	34
20	30	49	56	40	40	60	55	67	48
20	40	53	66	52	40	70	52	68	55
20	50	48	64	54	50	60	40	57	27
30	40	46	56	36	50	70	55	68	48
30	50	56	68	51	50	80	43	69	57
30	60	49	65	55	60	65	11	15	0.7
40	43	13	15	0.5					

Table 2: Efficiencies in percent for $\tilde{\chi}^0_1\tilde{\chi}^0_2$ events with different decays modes of $\tilde{\chi}^0_2$ and for different neutralino masses. Systematic errors are about $\pm 2\%$ absolute.

the region of the $(M_{\tilde{\chi}^0_2}, M_{\tilde{\chi}^0_1})$ plane where it would be kinematically possible for such an event to arise (approximately given by $M_{\tilde{\chi}^0_2} < 80$ GeV/c^2). The limits obtained are shown in Figs. 2a and 2b for the leptonic and hadronic $\tilde{\chi}^0_2$ decay modes. The limit obtained assuming that $\tilde{\chi}^0_2 \to f\bar{f}\ \tilde{\chi}^0_1$ decay is mediated by Z^{0*}, including both leptonic and hadronic modes and 20% of invisible final states, is presented in Fig. 2c.

In the $\tilde{\chi}^0_2\tilde{\chi}^0_2$ channel, 34000 events were generated and passed through the simulation and selection procedure, giving the efficiencies shown in Table 3. The limits obtained are shown in Fig. 2d-f for the same three assumptions on the $\tilde{\chi}^0_2$ decay mode.

Mass (GeV/c^2)		Efficiency (%)		Mass (GeV/c^2)		Efficiency (%)	
$M_{\tilde{\chi}^0_1}$	$M_{\tilde{\chi}^0_2}$	$\ell^+\ell^-\ell'^+\ell'^-$	$\ell^+\ell^-$ q$\bar{\text{q}}$; q$\bar{\text{q}}$q$\bar{\text{q}}$	$M_{\tilde{\chi}^0_1}$	$M_{\tilde{\chi}^0_2}$	$\ell^+\ell^-\ell'^+\ell'^-$	$\ell^+\ell^-$ q$\bar{\text{q}}$; q$\bar{\text{q}}$q$\bar{\text{q}}$
15	18	31	2	30	65	67	47
15	25	55	29	50	53	14	1
15	43	50	37	50	55	44	16
15	65	53	33	50	65	67	55
30	33	27	3	60	63	15	1
30	45	65	43	60	65	47	12

Table 3: Efficiencies in percent for $\tilde{\chi}^0_2\tilde{\chi}^0_2$ events for different visible final states and for different neutralino masses. Systematic errors are about $\pm 2.5\%$ absolute.

These results were interpreted in terms of the MSSM with universal GUT scale parameters by evaluating the appropriate efficiency, cross section, and branching ratio for each channel as functions of M_2, μ, and $\tan\beta$. Exclusion regions were derived by comparing the expected number of events with the number actually observed and the number expected from background, using Poisson statistics in the Bayesian approach for combining the different channels [22].

Figure 3 shows the resulting limits in the (μ, M_2) plane for four different values of $\tan\beta$ and for different values of the universal scalar mass at the GUT scale, m_0. The

effect of changing m_0, and hence the mass of the scalar electron, is noticeable only for low M_2, and only in regions already excluded by lower energy LEP results.

For values of M_2 below about 100 GeV/c^2, the cross section for $\tilde{\chi}_1^0\tilde{\chi}_2^0$ production drops sharply. However, it is replaced by a significant cross section for $\tilde{\chi}_1^0\tilde{\chi}_3^0$, where the properties and branching ratios of $\tilde{\chi}_3^0$ are similar to those of $\tilde{\chi}_2^0$ for higher M_2. The exclusion region was extended to lower values of M_2, based on the calculated efficiencies for $\tilde{\chi}_1^0\tilde{\chi}_2^0$. For lower values of M_2, other $\tilde{\chi}_i^0\tilde{\chi}_j^0$ combinations with cascade decays involving photons become important.

5.2 Results on scalar lepton production

The efficiency of the selection in section 4.4 for scalar electron production, calculated using 4000 events for different mass combinations, is shown in Table 4. In the $\tilde{\mathrm{e}}$ case there is the additional possibility of $\tilde{\chi}_1^0$ exchange in the t-channel. In the case of low $|\mu|$ values, the t-channel and s-channel contributions may interfere destructively, giving cross sections of about 0.5 pb for $M_{\tilde{\mathrm{e}}} = 40$ GeV/c^2. For larger $|\mu|$, however, meaningful limits may be set.

Figure 6a shows the excluded regions for production of $\tilde{\mathrm{e}}_R^+\tilde{\mathrm{e}}_R^-$ only (assuming a heavy $\tilde{\mathrm{e}}_L$), and Fig.6b shows those for production of $\tilde{\mathrm{e}}_R^+\tilde{\mathrm{e}}_R^-$, $\tilde{\mathrm{e}}_L^+\tilde{\mathrm{e}}_L^-$, and $\tilde{\mathrm{e}}_R^+\tilde{\mathrm{e}}_L^-$ with $M_{\tilde{\mathrm{e}}_L} = M_{\tilde{\mathrm{e}}_R}$. These limits apply for 200 GeV/c^2 $< |\mu| <$ 1 TeV/c^2 and $1 < \tan\beta < 50$, and are computed taking into account the candidate event described in section 4.4.

Mass (GeV/c^2)		Efficiency (%)			Mass (GeV/c^2)		Efficiency (%)		
$M_{\tilde{\chi}_1^0}$	$M_{\tilde{\mathrm{f}}}$	$\tilde{\mathrm{e}}\tilde{\mathrm{e}}$	$\tilde{\mu}\tilde{\mu}$	$\tilde{\mathrm{t}}\tilde{\mathrm{t}}$	$M_{\tilde{\chi}_1^0}$	$M_{\tilde{\mathrm{f}}}$	$\tilde{\mathrm{e}}\tilde{\mathrm{e}}$	$\tilde{\mu}\tilde{\mu}$	$\tilde{\mathrm{t}}\tilde{\mathrm{t}}$
20	50	42	56	51	47	50	19	33	15
20	60	46	64	46	50	60	57	67	50
20	65	49	65	60	57	60	17	24	4
40	50	50	65	55	57	65	49	62	40
40	60	51	65	60	60	65	44	53	29

Table 4: Efficiencies in percent for $\tilde{\mathrm{f}}\bar{\tilde{\mathrm{f}}}$ events for different sfermion types and for different $\tilde{\mathrm{f}}$ and $\tilde{\chi}_1^0$ masses. Systematic errors are about ±3.5% absolute.

The search of section 4.4 yielded no events with $\mu\mu$ final states. The selection efficiency for scalar muons was evaluated using fully simulated samples generated with `SUSYGEN` (a total of 4000 events for different mass combinations) and is also shown in Table 4. Two cases were considered, namely the case of degenerate masses, $M_{\tilde{\mu}_R} = M_{\tilde{\mu}_L}$, and the case of a lighter $\tilde{\mu}_R$ and a kinematically inaccessible $\tilde{\mu}_L$, as suggested by the running of scalar mass terms in the MSSM. The limit improves on previous LEP1 limits only in the mass degenerate case, for which the excluded region is shown in Fig. 6c.

5.3 Results on scalar quark production

The expected cross section for scalar top quark production is in the picobarn range close to the kinematic limit, but may be reduced if left-right mixing causes decoupling from the Z^0 in the s-channel, leaving only the photon contribution.

The sensitivity of the selection of acoplanar jet events described in section 4.1 to $\tilde{t}$ production was evaluated using fully simulated event samples for several $(M_{\tilde{t}}, M_{\tilde{\chi}^0_1})$ combinations, supplemented by a large set of generator data passed through a very fast detector response parametrization to interpolate results obtained with the full simulation. Table 4 shows the efficiency of the selection for different mass combinations. Figure 6d shows the mass combinations excluded at the 95% confidence level, together with results from previous searches at LEP1 [23] and the Tevatron [24]. The results are shown for the left and right stop quarks. An analysis similar to the one described in section 4.2 gave similar results.

The expected cross-section for $\tilde{b}_L\bar{\tilde{b}}_L$ production is about 2 pb for $M_{\tilde{b}} = 50$ GeV/c^2. To search for this process, the analysis of section 4.2 was applied. The efficiencies for different mass combinations were calculated using a total of 27000 fully simulated events. They were found to be close to 50% for a difference in mass between $\tilde{b}_L$ and $\tilde{\chi}^0_1$ above approximately 10 GeV. Although the analysis gave no evidence for $\tilde{b}_L$ production, the selected event was treated as a candidate, giving exclusion limits in the $(M_{\tilde{b}L}, M_{\tilde{\chi}^0_1})$ plane as shown in figure 6d.

6 Conclusions

In a data sample of 5.9 pb^{-1} collected by the DELPHI detector at centre-of-mass energies of 130 and 136 GeV, searches were performed for events with acoplanar jet pairs, acoplanar lepton pairs, or combinations of these, in association with missing energy. One event was selected (see section 4.4): an acoplanar pair of electrons with momenta 7.6 GeV/c and 11.6 GeV/c and an invariant mass of 4.6 GeV/c^2, consistent with the expected number of background events of 1.3$\pm$0.9 and in particular with the 0.6 ± 0.3 expected from $e^+e^- \to \ell^+\ell^-\nu\bar{\nu}$. There was no candidate in the acoplanar jets topology. The specific sbottom search led to one candidate event, described in section 4.2, with 2.4 ± 0.5 events expected from background. These results are used to set limits on the production of neutralinos, scalar leptons, and scalar quarks, and consequently on the parameters of the MSSM, as shown in Figs. 2-4.

Assuming the dominant decay of $\tilde{\chi}^0_2$ into $\tilde{\chi}^0_1$ and a virtual Z^0, the cross section for $\tilde{\chi}^0_1\tilde{\chi}^0_2$ production is limited to be below a few picobarns at the 95% confidence level in most of the kinematically allowed mass range (see Fig. 2).

If the gaugino mass parameter M_2 is in the region between 150 GeV/c^2 and 400 GeV/c^2 (Higgsino dominated case) the Higgs superfield mass parameter, μ, is excluded in the region -45 GeV/$c^2 < \mu < 80$ GeV/c^2 for $\tan\beta$=1.0 and $|\mu| < 65$ GeV/c^2 for $\tan\beta$=35, independent of the m_0 value. A narrow window for μ close to zero that is not covered in this analysis is covered by previous LEP1 searches (see Fig. 3).

In the case of degenerate scalar electron masses, $M_{\tilde{e}_L} = M_{\tilde{e}_R}$, values below 56.5 GeV/$c^2$ are excluded at the 95% confidence level if $M_{\tilde{e}L,R} - M_{\tilde{\chi}^0_1} > 5$ GeV/c^2, 200 GeV/$c^2 < |\mu| <$ 1 TeV/c^2, and $\tan\beta > 1$ (Fig. 4b). For degenerate scalar muons the corresponding limit is 51 GeV/c^2, irrespective of the MSSM parameters (Fig. 4c).

The mass of the left scalar top quark, $M_{\tilde{t}_L}$, is limited to be above 56 GeV/c^2 at the 95% confidence level if it is at least 8 GeV/c^2 heavier than the lightest neutralino (Fig.4d). The left sbottom mass, $M_{\tilde{b}L}$, is constrained to be above 53 GeV/c^2 at 95% confidence level if it is at least 20 GeV/c^2 above $M_{\tilde{\chi}^0_1}$ (also Fig. 4d).

These results extend exclusion limits obtained at LEP1, and probe a relevant part of the MSSM parameter space.

Acknowledgements

We express our gratitude to the members of the CERN accelerator divisons and compliment them on the fast and efficient comissioning and operation of the LEP accelerator in this new energy regime.

References

[1] H.P. Nilles, Phys. Rep. **110** (1984) 1;
H.E. Haber and G. L.Kane, Phys. Rep. **117** (1985) 75.

[2] ALEPH Collaboration: D. Decamp *et al.*, Phys. Rep. **216** (1992) 253;
A. Lopez-Fernandez, "*Search for Z^0 decays into sleptons and neutralinos using the DELPHI detector*", DELPHI note 92-95 (Dallas) PHYS 206;
L3 Collaboration: M. Acciarri *et al.*, Phys. Lett. **B350** (1995) 109;
OPAL Collab: G.Alexander *et al.*, "*Topological search for the production of neutralinos and scalar particles*", CERN PPE/96-019, February 1996, to be published in Phys. Lett. B.

[3] M. Drees and K. Hikasa, Phys. Lett. **B252** (1990) 127.

[4] The LEP Collaborations: ALEPH, DELPHI, L3, OPAL, "*A combination of preliminary LEP electroweak measurements and constraints on the Standard Model*", CERN PPE/95-172, November 1995.

[5] G. Altarelli and R. Barbieri, Phys. Lett. **B253** (1990) 161;
M. Boulware and D. Finnell, Phys. Rev. **D44** (1991) 2054;
A. Djouadi *et al.*, *Nuclear Physics* **B349** (1991) 48.

[6] DELPHI Collaboration: P. Abreu *et al.* "*Search for the lightest chargino at $\sqrt{s} = 130$ and 136 GeV*", CERN PPE/96-75, June 1996, to be published in Phys. Lett. B.

[7] ALEPH Collaboration: D. Buskulic *et al.*, Phys. Lett. **B373** (1996) 246;
L3 Collaboration: M. Acciarri *et al*, "*Search for Supersymmetric Particles at 130 GeV $< \sqrt{s} <$ 140 GeV at LEP*", CERN PPE/96-029, February 1996, subm. to Phys. Lett. B;
OPAL Collaboration: G. Alexander *et al*, "*Search for Chargino and Neutralino Production Using the OPAL Detector at $\sqrt{s} = 130 - 136$ GeV*", CERN PPE/96-020, February 1996, to be published in Phys. Lett. B.

[8] DELPHI Collaboration: P. Abreu *et al.* Nucl. Instr. and Meth. **A378** (1996) 57.

[9] T. Sjöstrand, Comp. Phys. Comm. **39** (1986) 347; T. Sjöstrand, "`PYTHIA 5.6` *and* `JETSET 7.3`", CERN-TH/6488-92.

[10] S.Katsanevas and S.Melachroinos in "*Physics at LEP2*", CERN 96-01, Vol.2, p.328.

[11] S. Ambrosanio and B. Mele, Phys. Rev. **D52** (1995) 3900;
S. Ambrosanio and B. Mele, Phys. Rev. **D53** (1996) 2451.

[12] S. Kawabata, Comp. Phys. Comm. **41** (1986) 127.

[13] W. Beenakker, R. Hopker, M. Spira, and P.M. Zerwas, Phys. Lett. **B349** (1995) 463.

[14] Working group on event generators for discovery physics: M.L.Mangano and G.Ridolfi (conveners), in "*Physics at LEP2*", CERN 96-01, Vol.2, p.340.

[15] F.A. Berends, R. Pittau, R. Kleiss, Comp. Phys. Comm. **85** (1995) 437.

[16] S. Nova, A. Olshevski, and T. Todorov, *A Monte Carlo event generator for two photon physics*, DELPHI note 90-35 PROG 152.

[17] S. Bethke *et al.*, Phys. Lett. **B213** (1988) 235.

[18] K. Hikasa and J. Hisano, "*Hard gluon emission from colored scalar pairs in e^+e^- annihilation*" TU-497, TIT-HEP-308, March 1996, to be published in Phys. Rev. D.

[19] M.G. Kendall and A. Stuart, *The advanced theory of statistics*, (Griffin, London 1966);
R.A. Fisher, "*The use of multiple measurements in taxonomic problems*", *Annals of Eugenics*, **7**(1936).
[20] G.C. Fox and S. Wolfram, Nucl.Phys. **B149** (1979) 413.
[21] Particle Data Group: L.Montanet *et al.*, Phys. Rev. **D50** (1994) 1173.
[22] V.F. Obraztsov, Nucl. Instr. and Meth. **316** (1992) 388.
[23] The OPAL Collaboration: R. Akers *et al.*, Phys. Lett. **B337** (1994) 207.
[24] D0 Collaboration: S. Abachi *et al.*, Phys. Rev. Lett. **76** (1996) 2222.
[25] ALEPH Collaboration: D. Decamp *et al.* Phys. Rep. **216** (1992) 253;
DELPHI Collaboration: P. Abreau *et al.* Phys. Lett. **B247** (1990) 157;
L3 Collaboration: O. Adriani *et al.* Phys. Rep. **236** (1993) 1;
OPAL Collaboration: M.Z. Akrawy *et al.* Phys. Lett. **B240** (1990) 261.
[26] ASP Collaboration: C. Hearty *et al.* Phys. Rev. **D39** (1989) 3207

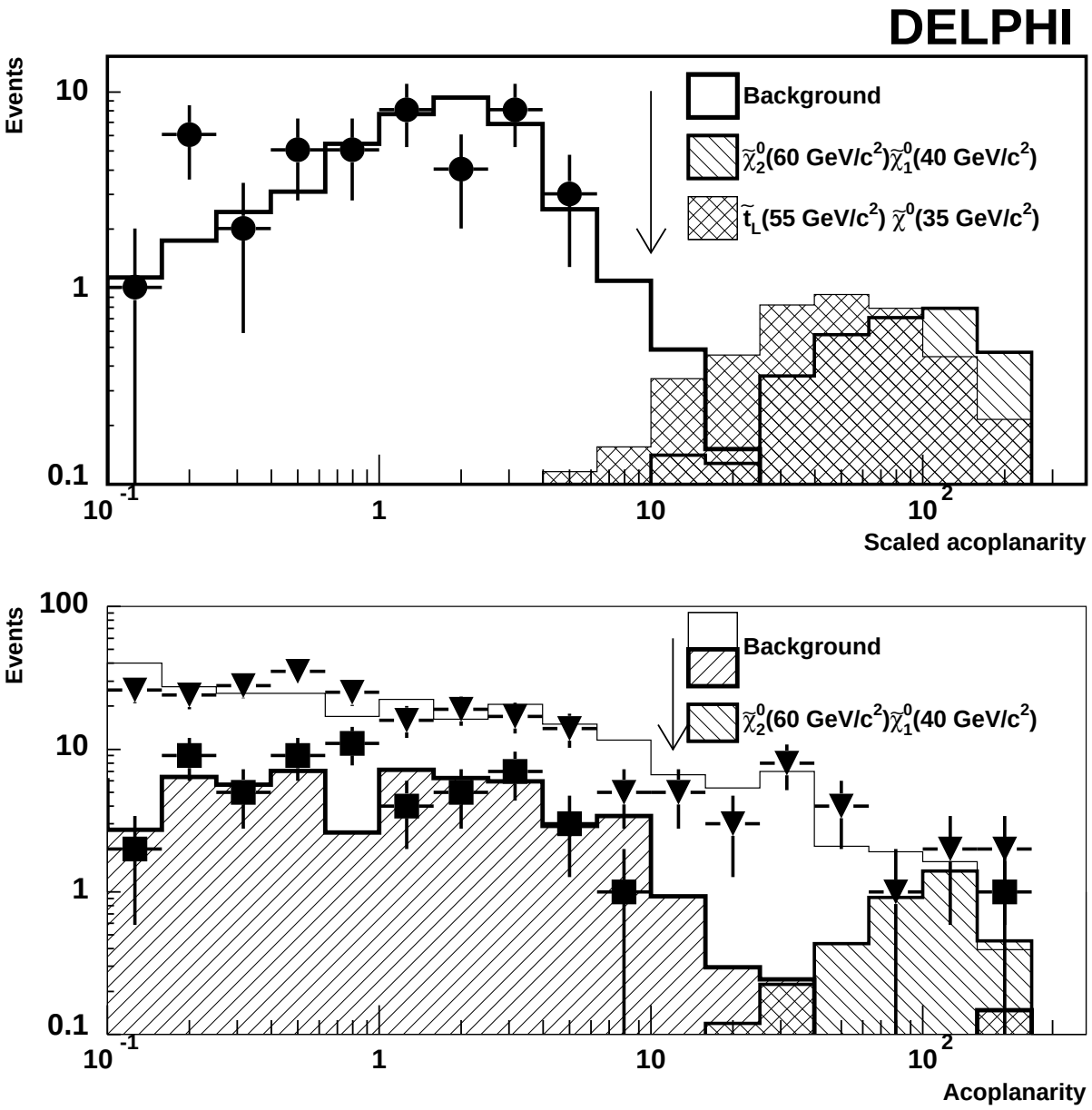

Figure 1: The upper plot shows the distribution of scaled acoplanarity (see text) for the hadronic events in the data (circles), compared to the simulation of the background (unhatched histogram) before this variable was used in the final selection step of section 4.1. The hatched and cross-hatched histogram show the expected distributions the $\tilde{\chi}_1^0\tilde{\chi}_2^0$ and $\tilde{t}_L\bar{\tilde{t}}_L$ signals, normalised to cross sections of 1 pb and 1.2 pb, respectively. The lower plot shows the acoplanarity distribution for leptonic real data events (triangles and squares) and the simulated background events (unhatched and hatched histograms peaking at low values) which pass two different selections. The triangles and the unhatched histogram show all low multiplicity events with missing transverse momentum above 4 GeV/c and two well reconstructed tracks, while the squares and the hatched histogram show the events which survive all steps in the selection of section 4.4 prior to the final requirements on acoplanarity and acollinearity. The distribution expected in the latter case for simulated neutralino events, normalised to a cross section of 1 pb, is shown by the differently hatched histogram which peaks at high values of the acoplanarity. The arrows indicate the final selections applied.

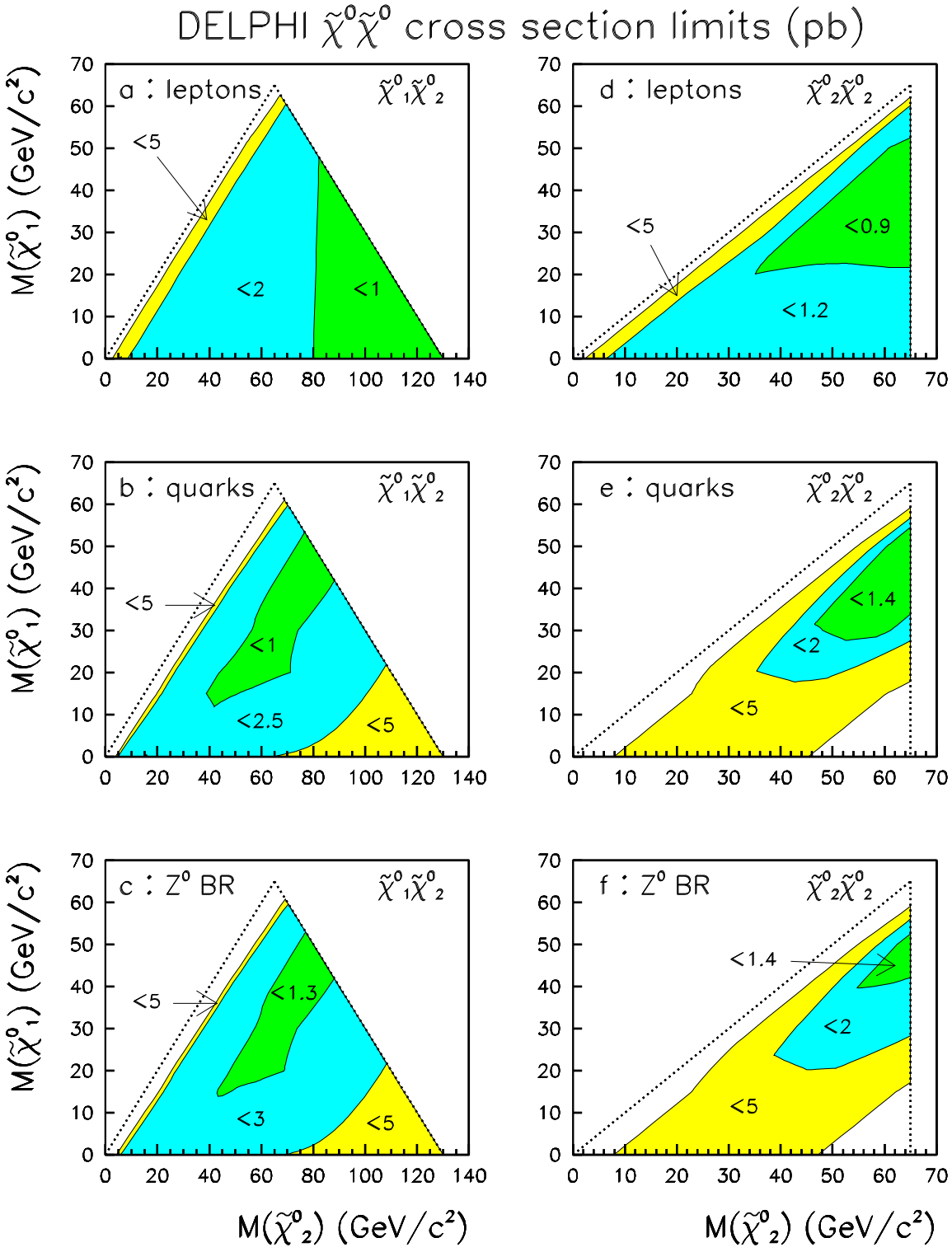

Figure 2: Upper limits on the cross sections in picobarns at the 95% confidence level for $\tilde{\chi}^0_1\tilde{\chi}^0_2$ production (**a-c**) and $\tilde{\chi}^0_2\tilde{\chi}^0_2$ production (**d-f**). For the upper figures (**a, d**), $\tilde{\chi}^0_2$ decays into $\tilde{\chi}^0_1 e^+e^-$and $\tilde{\chi}^0_1\mu^+\mu^-$ were assumed to dominate. For (**b, e**) the dominant mode was assumed to be $\tilde{\chi}^0_1 q\bar{q}$. For the lower figures (**c, f**), the $\tilde{\chi}^0_2$ was assumed to decay into $\tilde{\chi}^0_1 f\bar{f}$ with the same branching ratios into different fermion flavours as the Z^0. The dotted lines indicate the kinematic limits.

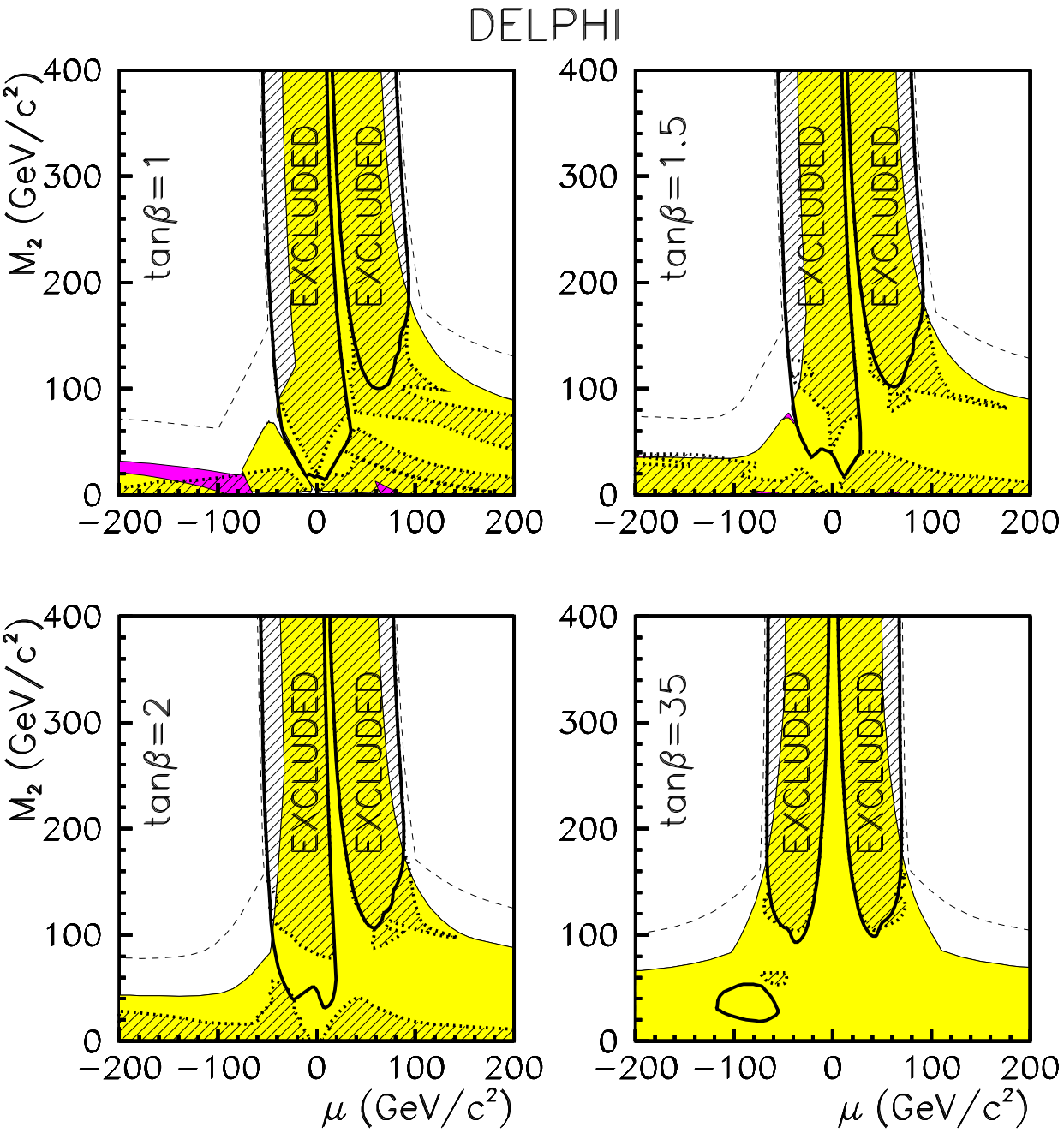

Figure 3: Regions in the (μ, M_2) plane excluded at 95% confidence for different values of $\tan\beta$. The thick solid lines correspond to m_0=1 TeV/c^2 and the hatched areas enclosed by dotted lines to 30 GeV/c^2. The lightly shaded areas show the regions excluded by LEP 1 for m_0=1 TeV/c^2, while the more heavily shaded area is excluded only for m_0=30 GeV/c^2. The thin dashed line shows the kinematic limit for $\tilde{\chi}^0_1\tilde{\chi}^0_2$ production at $E_{\rm cms}$ =136 GeV.

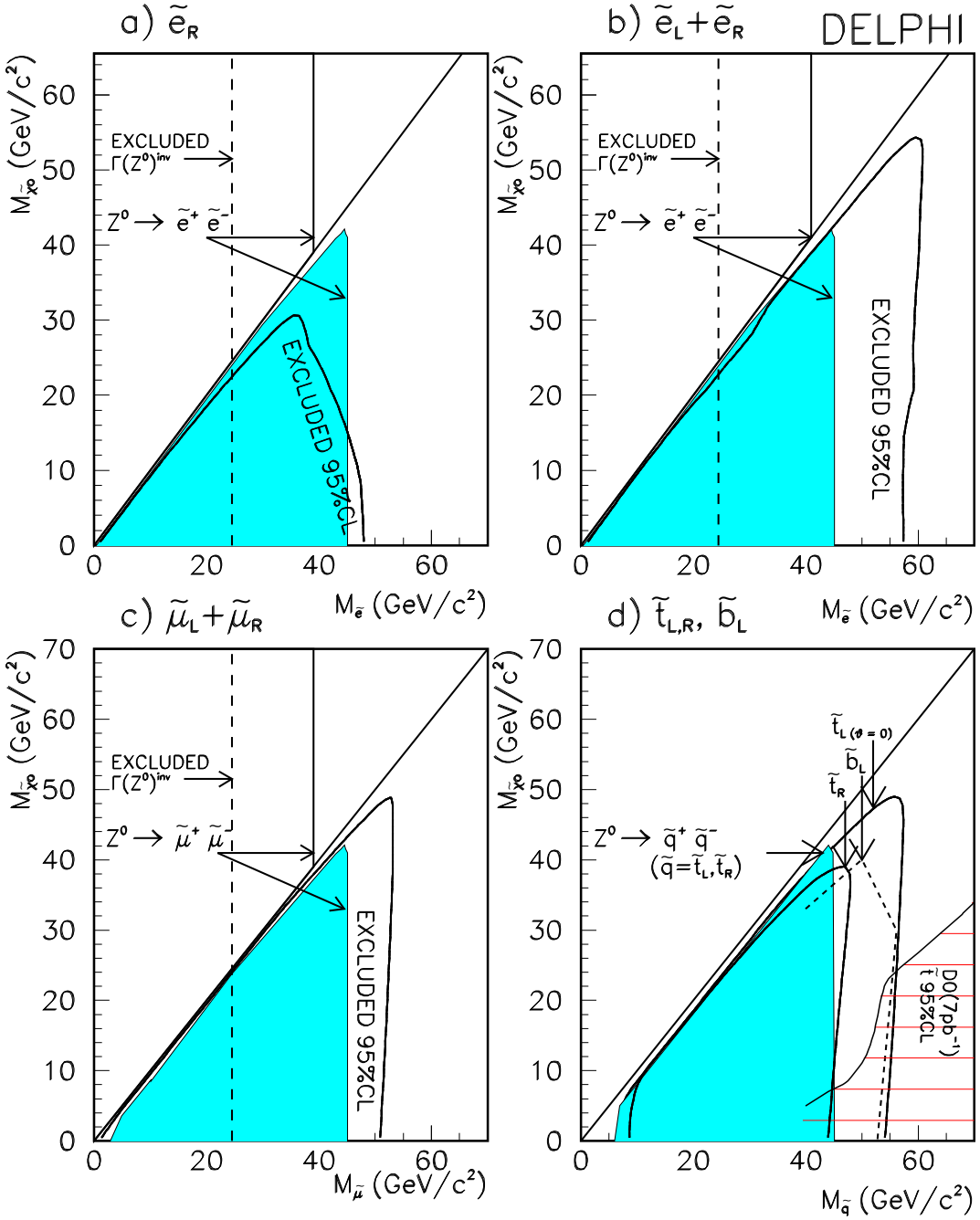

Figure 4: Exclusion regions in the $(M_{\tilde{f}}, M_{\tilde{\chi}^0_1})$ planes for **a)** $\tilde{e}_R$, **b)** degenerate $\tilde{e}_R\tilde{e}_L$ **c)** degenerate $\tilde{\mu}_R\tilde{\mu}_L$. LEP1 limits coming from direct searches (shaded areas and vertical solid lines) and the Z^0 invisible width measurement (vertical dashed line) are also shown [25]. The area above the diagonal corresponds to a stable $\tilde{f}$. Limits for $\tilde{t}_R$, $\tilde{t}_L$ and $\tilde{b}_L$ are shown in **d)** together with Tevatron limits [24] for $\tilde{t}$ (hatched area); the LEP1 limit for $\tilde{b}_L$ is close to that for $\tilde{t}$ (shaded area). There are further limits for scalar electrons from single photon searches at earlier e^+e^- colliders [26] which exclude $M_{\tilde{e}R} < 53\mathrm{GeV}/c^2$ and degenerate $M_{\tilde{e}R,L} < 65\mathrm{GeV}/c^2$ under the assumption that the lightest supersymmetric particle, $\tilde{\chi}^0_1$, is a nearly massless photino. All limits given are at 95% confidence level.